WATER RESOURCES RESEARCH, VOL. 35, NO. 6, PAGES 1761–1770, JUNE 1999

Three-dimensional hydrofacies modeling based on soil surveys and transition probability geostatistics

Gary S. Weissmann, Steven F. Carle,[1] and Graham E. Fogg[2]
Hydrologic Sciences, University of California, Davis

Abstract. Typical hydrogeologic data sets consisting of information from boreholes provide excellent information on vertical variability of sedimentary deposits but very limited information on lateral distribution and variability. In cases where surface geomorphic features reflect processes similar to those responsible for past deposition, the soil survey offers a resource for assessing the lateral sediment variability. Facies mean length and transition probability measurements of C horizon textures from the soil maps on the Kings River alluvial fan, California, provide a basis for Markov chain models of spatial variability in the principal lateral directions and facies orientation information for the horizontal plane. Incorporation with a Markov chain model of vertical-direction transitions based on well data yields a three-dimensional Markov chain model of sediment variability which includes cross correlation between sediment types and representation of asymmetry (e.g., fining upward tendencies). Use of the model in geostatistical conditional simulation and simulated annealing produces a detailed, geologically plausible image of the subsurface hydrofacies distribution.

1. Introduction

The difficulty of characterizing subsurface heterogeneity with commonly sparse data sets severely limits the accuracy and realism of transport models. A typical hydrogeologic or petroleum data set consists of wire line logs, driller's lithologic logs, and limited core from widely spaced wells. These data may provide excellent information on the vertical variability of the sediments but only limited information about the lateral distribution and variability of the deposits.

Numerous characterization methods have been proposed for modeling the spatial distribution of hydrostratigraphic material in light of this limited lateral variability information. *Koltermann and Gorelick* [1996] classified these methods as either descriptive, process imitating, or structure imitating. The descriptive methods use site specific information, such as well logs and geophysical data, along with a conceptual geologic model to divide the aquifer into characteristic hydrogeologic zones; however, the conversion of descriptive models to a quantitative hydrostratigraphic model is often difficult and unclear, as is quantification of uncertainty [*Koltermann and Gorelick*, 1996]. Surface geophysical methods [e.g., *Bashore et al.*, 1994] such as seismic reflection surveys and ground-penetrating radar show great promise, but relating geophysical attributes to hydraulic properties remains difficult.

Process-imitating models attempt to mimic the complex distribution of facies by simulating the accumulation of sediments in depositional sequences. However, these methods do not honor actual data at well locations and may not contain sufficient site specific information [*North*, 1996; *Koltermann and Gorelick*, 1996]. Additionally, the process models are computationally demanding and highly sensitive to initial conditions, boundary conditions, and calibration to tectonic and climatic histories for which appropriate data and interpretation are subjective and difficult to obtain [*Koltermann and Gorelick*, 1996].

Structure-imitating methods, commonly based on geostatistics, honor known data points and patterns of spatial variability [*Deutsch and Journel*, 1992; *Carle*, 1996]. However, the development of a model of lateral spatial variability (e.g., variogram) tends to be problematic and uncertain because lateral continuity of geologic facies is usually significantly smaller than spacing between wells in heterogeneous porous media. Fusion of geophysical, geostatistical, and hydrologic data can greatly improve the variogram model and resulting characterization [*McKenna and Poeter*, 1995; *Hyndman and Gorelick*, 1996], but knowledge of lateral variability usually remains substantially more uncertain than the knowledge of vertical variability.

The use of previously recorded C horizon (approximately 1.5 m depth) soil data may provide considerable insight for deriving geostatistical correlation structure in undersampled, lateral directions, assuming that the modern geomorphologic processes are similar to those responsible for formation of the aquifer system. In these cases the soil survey may be used as a "training image" [*Deutsch and Journel*, 1992; *Koltermann and Gorelick*, 1996] for understanding the spatial distribution of facies in lateral directions. We present a new application of soil survey data in conjunction with subsurface data (e.g., well logs and core) and a structure-imitating method that employs a transition probability and Markov chain geostatistical approach to create geologically plausible, three-dimensional characterizations of a heterogeneous, fluvial aquifer system. The example application shows how the geostatistical technique facilitates joint incorporation of soil data, well log data, and geologic interpretation into development of a three-dimensional model of hydrofacies architecture.

[1]Now at Lawrence Livermore National Laboratory, Livermore, California.
[2]Also at Department of Geology, University of California, Davis.

Copyright 1999 by the American Geophysical Union.

Paper number 1999WR900048.
0043-1397/99/1999WR900048$09.00

Figure 1. Map of California showing the location of the Kings River alluvial fan study area.

2. Geologic Framework and Data

The Kings River alluvial fan aquifer system provides an excellent location for integration of soil survey data into a three-dimensional model of subsurface heterogeneity. The aquifer system consists of unconsolidated sediments deposited on a stream-dominated alluvial fan that developed where the Kings River exits the Sierra Nevada mountains into the San Joaquin Valley (Figure 1). The alluvial fan deposits consist of channel gravels and sands embedded within finer-grained floodplain and levee deposits.

A high-quality soil survey for this study area, produced by the U.S. Department of Agriculture [*Huntington*, 1971], shows the lateral spatial distributions of geologic facies on the fan surface. As the last of a series of soil surveys in the region, this survey represents a culmination of geomorphic understanding about this alluvial fan system, where soil profiles were interpreted and matched to geomorphic characteristics of the alluvial fan depositional environments [*Huntington*, 1980]. The compilation of the soil survey included soil profiles to depths of up to 2 m and field data records from over 40,000 surface and shallow subsurface borings, special excavations, road cuts, and natural exposures in the eastern Fresno County study area [*Huntington*, 1980]. Consequently, these soil maps contain detailed, regional descriptions of the spatial patterns in recent depositional facies.

Subsurface data from the study area include approximately 150 m of core from three wells and wire line logs from seven wells to depths up to 82 m collected by the U.S. Geological Survey (USGS) [*Burrow et al.*, 1997] and approximately 150 m of continuous core obtained from 22 shallow test holes drilled along transects to depths of approximately 10 m. These transects enabled comparison of the soil survey data to deeper intervals with regard to subsurface lateral variability.

On the basis of core data, sediments were categorized into four hydrofacies: gravel, sand, muddy sand, and mud, where "mud" refers to undifferentiated silt and clay (Table 1). The volumetric proportions listed in Table 1 represent the fraction of each hydrofacies encountered in the USGS core. The gravel and sand facies form the aquifer, while the muddy sand and mud form aquitard bodies.

The gravel facies consists of small cobbles and pebbles in a matrix of coarse to very coarse sand attributed to channel lag deposits of the ancestral Kings River. The gravel facies tends to occur below the sand facies and, lacking in silt and clay, likely possesses the highest hydraulic conductivity in the sedimentary sequence. The sand facies consists of medium- to coarse-grained sand that was deposited primarily in channels of the Kings River or secondary distributary channels on the alluvial fan. The muddy sand facies consists of finer-grained sand that may include a matrix of clay and silt. This hydrofacies includes bar top sediments within the upper portions of channel deposits and levee or proximal floodplain deposits. Orange to reddish coloration, root traces, and evidence of translocated clays in some of these deposits indicate slight to moderate pedogenic alteration due to relatively short-duration surface exposure. The mud facies corresponds to distal floodplain deposits consisting of massive to laminated silt and mud with occasional fine sand laminae. Some mud facies show evidence of relatively intense pedogenic alteration, as indicated by red coloration, root traces, and thick coats of translocated clay on grains and ped (soil structures) faces. These buried soils are attributed to extended periods of landscape stability on the alluvial fan surface [*Lettis*, 1988]. These facies are consistent with stream-dominated alluvial fan deposition.

Identification and correlation of these subsurface facies to C horizon textures recorded in the soil survey provide indications of the lateral distribution of these facies in the deeper subsurface. The soil survey lists type profile descriptions for each soil series (e.g., soil types). Subtle variations in soil series textures are described in the survey as "mappable units." The C horizon texture described for each mappable unit were categorized into the appropriate subsurface hydrofacies based on textures, as shown in Table 1. For example, soil textures dominated by

Table 1. Hydrostratigraphic Facies Defined for the Kings River Alluvial Fan Aquifer System From Core and Soil Survey Interpretations

Hydrofacies	Geologic Interpretation	C Horizon Texture	Volumetric Proportions
gravel	channel lag gravel	···	0.03
sand	channel bar sand	sand, loamy sand	0.46
muddy sand	bar top, levee, proximal overbank	(fine) sandy loam	0.26
mud	overbank fines, paleosols	clay, silt, clay loam, hardpan	0.25

Ellipsis indicates this texture was not present on the soil survey.

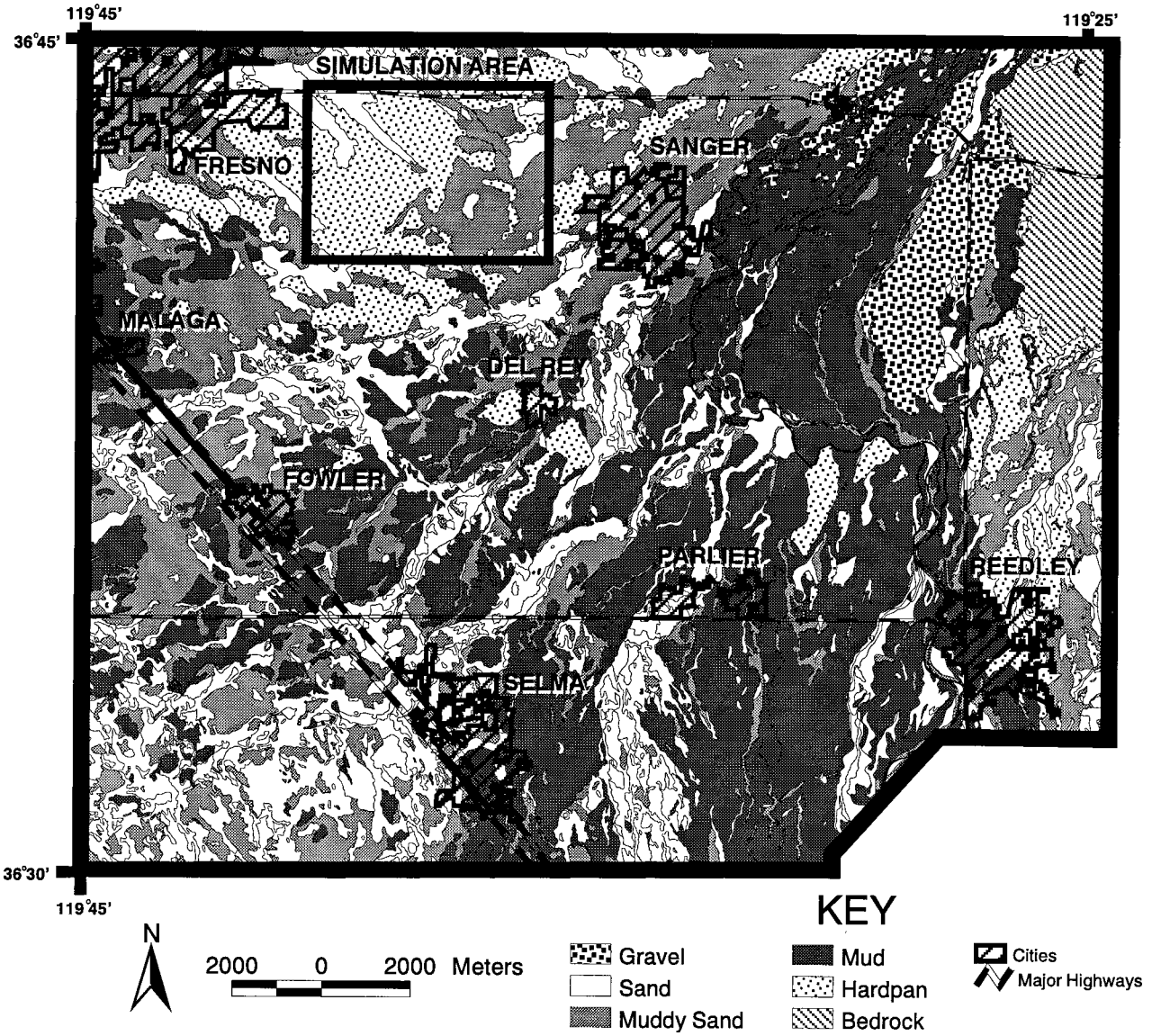

Figure 2. A map of the geomorphic distribution of hydrofacies based upon a classification of the C horizon textures as listed in Table 1 [modified from *Huntington*, 1971]. This map clearly shows the orientation and distribution of various facies on the Kings River alluvial fan.

sand (e.g., sand or loamy sand) were included in the sand facies. By replotting the soil survey based on these categories, a map of the surface distribution of hydrofacies was produced (Figure 2). The C horizon textures are used because these most closely reflect the unaltered textures of sediment deposited on the alluvial fan. Additionally, since the C horizon occurs at depths of 1.5 to 2 m, the map represents textures that are not influenced by plowing or other anthropogenic effects.

This map shows the characteristic alluvial fan radial pattern of coarse-grained channels which are surrounded by finer-grained floodplain deposits, where channel cross sections or lengths are longer in the depositional dip direction (parallel to channel axis orientation) and shorter in the depositional strike direction (perpendicular to the channel axis). Because the processes that deposited the sediments reflected by the soil survey are the same as those responsible for aquifer deposition [*Lettis*, 1988], similar lateral facies distribution patterns are expected in the subsurface.

3. Geostatistics and Geology

In the water resources literature, geostatistical modeling of subsurface spatial structure has been performed using approaches based on continuous random functions [e.g., *Gelhar and Axness*, 1983; *Dagan*, 1989; *Neuman and Zhang*, 1996] and indicator-based methods for categorical variables [e.g., *Johnson and Driess*, 1989; *Desbarats*, 1993; *Ritzi et al.*, 1995; *McKenna and Poeter*, 1994, 1995]. In both approaches a variogram or covariance function is used as the model of spatial variability. Estimation of spatial structure models of continuous random functions, such as hydraulic conductivity (K) for subsurface systems, is problematic because of the typically sparse measurements of K. Indicator methods have been attractive as a means of addressing the categorical nature of geologic data and for incorporating the geometric context of geologic facies. Nevertheless, geologic information tends to be too sparse in the lateral directions to support direct inference of horizontal

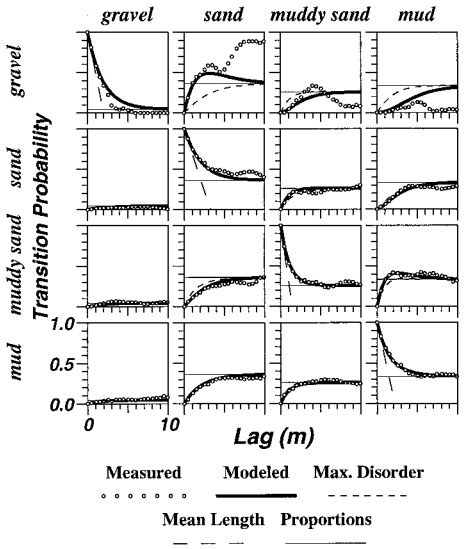

Figure 3. Matrix of vertical-direction transition probabilities showing U.S. Geological Survey core data measurements (circles) and the Markov chain model (solid lines) for the Kings River alluvial fan. The fine solid horizontal lines indicate the sills which show the volumetric proportions of facies in each column. Intersection of the long-dashed line (tangent) with lag axes indicate mean lengths of each facies. The short-dashed lines show the maximum disorder transition probability, as described in the text.

indicator variograms, and significant questions remain about the ability of indicator variograms to represent basic characteristics of geologic facies assemblages [*Fogg et al.*, 1998]. For example, geologic facies inherently exhibit different geometries and cross correlation and have proven difficult to represent and model with past indicator approaches, especially when the number of categories or facies exceeds two [*Deutsch and Journel*, 1992]. Furthermore, if data are too sparse to directly determine indicator variogram models, one must use geologic principles and concepts to synthesize appropriate models. Practical means of accomplishing this with traditional indicator methods, such that the relevant geologic features are preserved, have been little explored or demonstrated.

The use of a "training image," such as a geologist's conceptual drawing representing the general style of heterogeneity, can be useful for synthesizing an appropriate variogram model. Often, however, one may wish to estimate the spatial correlation function using outcrop descriptions or soil maps as analogs for the actual system of interest. Inevitably, the resulting function must be adjusted to represent the differing characteristics occurring in the subsurface system relative to the analog, such as differing volumetric proportions, mean lengths, and juxtapositional tendencies of the facies. Recognizing and adjusting the quantitative manifestations of these features in (cross) variograms or (cross) covariances is difficult. Furthermore, cross variograms cannot represent the asymmetrical correlation structures commonly observed in geologic systems (e.g., fining upward sequences) [*Carle and Fogg*, 1996; *Fogg et al.*, 1998], and practical, proven techniques for modeling cross covariances in a geologic system containing more than two categories (facies) have not been developed.

Below, we briefly describe an approach based on transition probability geostatistics using the vertical data to illustrate model development and geologic inputs into the model. Details of this technique are given by *Carle* [1996, 1997a, 1997b], *Carle and Fogg* [1996, 1997], and *Carle et al.* [1998]. Herein we present a new variation on the technique that involves use of embedded transition probabilities to develop the Markov chain model. We then show how the soil map is used to develop a three-dimensional model of spatial variability. This geostatistical approach provides the theoretical and practical framework for both representing the coregionalization structure of complex, cross-correlated hydrofacies assemblages and estimating this structure from a combination of hard data, analog models, and geologic concepts and principles.

4. Transition Probability/Markov Geostatistical Approach: Theory and Application

The transition probability/Markov chain approach to modeling spatial variability facilitates integration of geologic concepts and reduces reliance on the traditional empirical curve-fitting approach. Readily observable geologic attributes, including volumetric proportions, mean facies lengths (e.g., thickness and width), and juxtapositional tendencies, can be incorporated directly into development of a three-dimensional Markov chain model through a combination of fitting transition probability measurements and inference from geologic concepts and principles. The Markov chain model, in turn, is used in a cokriging procedure during conditional sequential indicator simulation and simulated quenching (zero-temperature annealing) [*Deutsch and Journel*, 1992] to generate "realizations" of subsurface facies distributions.

The transition probability $t_{jk}(\mathbf{h})$ is defined as

$$t_{jk}(\mathbf{h}) = \Pr\{k \text{ occurs at } \mathbf{x} + \mathbf{h} | j \text{ occurs at } \mathbf{x}\} \tag{1}$$

where k and j refer to categories or geologic facies, $\mathbf{x}$ is a spatial location vector, and $\mathbf{h}$ is a separation vector. Once vertical borehole data are categorized into facies, measurements of $t_{jk}(h_z)$ reflect the spatial continuity and juxtapositional tendencies of the facies. This is illustrated in Figure 3 where measurements of $t_{jk}(h_z)$ values from the core description show vertical (z) direction spatial relationships of the Kings River alluvial fan hydrofacies.

The bold solid line in Figure 3 represents a vertical Markov chain model calculated by the matrix exponential

$$\mathbf{T}(h_z) = \exp[\mathbf{R}_z h_z] \tag{2}$$

where $\mathbf{T}(h_z)$ denotes an $N \times N$ matrix of transition probabilities ($N = 4$ in Figure 3) and $\mathbf{R}_z$ is a matrix of transition rates for the vertical direction

$$\mathbf{R}_z = \begin{bmatrix} r_{11,z} & \cdots & r_{1N,z} \\ \vdots & \ddots & \vdots \\ r_{N1,z} & \cdots & r_{NN,z} \end{bmatrix} \tag{3}$$

with entries $r_{jk,z}$ describing the rate of change from category j to category k per unit length in the direction z. Differentiating (2) at $h_z = 0$, the transition rates are related to transition probabilities by

$$r_{jk,z} = \partial t_{jk}(0)/(\partial h_z) \tag{4}$$

[*Ross*, 1993; *Carle and Fogg*, 1997].

An eigenvalue analysis must be carried out in order to evaluate $\exp(\mathbf{R}_z h_z)$ because the matrix exponential is not com-

puted merely by computing the exponential of the matrix entries, that is, $t_{jk,z}(h_z) \neq \exp(r_{jk,z}h_z)$. Letting $h = h_z$ and $\mathbf{R} = \mathbf{R}_z$ for notational simplification, $\exp(\mathbf{R}h)$ is exactly determined by

$$\exp(\mathbf{R}h) = \sum_{i=1}^{N} \exp(\lambda_i h)\mathbf{S}_i \tag{5}$$

where λ_i and $\mathbf{S}_i$ denote the eigenvalues and spectral component matrices, respectively, of $\mathbf{R}$. The mathematical details are given by *Agterberg* [1974], *Carle and Fogg* [1997], and *Carle et al.* [1998]. One eigenvalue, say λ_i, is inherently zero and is associated with a spectral component matrix having the proportions along each column. Thus, for a four-category system the continuous lag Markov chain model written out completely consists of

$$\begin{aligned}\exp(Rh) = (1.0)&\begin{bmatrix} p_1 & p_2 & p_3 & p_4 \\ p_1 & p_2 & p_3 & p_4 \\ p_1 & p_2 & p_3 & p_4 \\ p_1 & p_2 & p_3 & p_4 \end{bmatrix} \\ &+ \exp(\lambda_2 h)\begin{bmatrix} s_{11,2} & s_{12,2} & s_{13,2} & s_{14,2} \\ s_{21,2} & s_{22,2} & s_{23,2} & s_{24,2} \\ s_{31,2} & s_{32,2} & s_{33,2} & s_{34,2} \\ s_{41,2} & s_{42,2} & s_{43,2} & s_{44,2} \end{bmatrix} \\ &+ \exp(\lambda_3 h)\begin{bmatrix} s_{11,3} & s_{12,3} & s_{13,3} & s_{14,3} \\ s_{21,3} & s_{22,3} & s_{23,3} & s_{24,3} \\ s_{31,3} & s_{32,3} & s_{33,3} & s_{34,3} \\ s_{41,3} & s_{42,3} & s_{43,3} & s_{44,3} \end{bmatrix} \\ &+ \exp(\lambda_4 h)\begin{bmatrix} s_{11,4} & s_{12,4} & s_{13,4} & s_{14,4} \\ s_{21,4} & s_{22,4} & s_{23,4} & s_{24,4} \\ s_{31,4} & s_{32,4} & s_{33,4} & s_{34,4} \\ s_{41,4} & s_{42,4} & s_{43,4} & s_{44,4} \end{bmatrix}\end{aligned} \tag{6}$$

where the $s_{\alpha\beta,i}$ are coefficients of the spectral component matrices $\mathbf{S}_i$ determined in the eigensystem analysis. Thus the Markov chain model for each entry $t_{jk}(h)$ in $\mathbf{T}(h)$ consists of a linear combination of $N - 1$ exponential structures added to the column category proportion. For example, in the four-category case given in (6)

$$\begin{aligned}t_{jk}(h) = p_k &+ s_{jk,2}\exp(\lambda_2 h) + s_{jk,3}\exp(\lambda_3 h) \\ &+ s_{jk,4}\exp(\lambda_4 h)\end{aligned} \tag{7}$$

In the case of the vertical direction transition probability matrix shown in Figure 3, the Markov chain model was fit to transition probability values measured in the USGS core based on observations at a 0.3 m spacing. Plots located in the main diagonal of Figure 3 represent autotransitions from a category to itself, and plots located off the main diagonal represent cross transitions from one category to another. The parameters of the Markov chain (e.g., the transition rates) reflect observable spatial attributes, including volumetric proportions, mean lengths (e.g., thicknesses), and facies juxtapositional tendencies. The ability to relate fundamental, observable attributes of the geologic system to parameters of the coregionalization model is vital to the application of a geostatistical method whether data are abundant or sparse. Below we describe the manifestations of volumetric proportions, mean lengths, and juxtaposition tendencies in the Markov chain model.

4.1. Volumetric Proportions

The "sills" of transition probability plots (i.e., values the transition probabilities tend toward with increasing lag), shown by the horizontal thin line in Figure 3, reflect volumetric proportions of the column categories and are thus related to the transition probabilities by

$$\lim_{h_\phi \to \infty} t_{jk}(h_\phi) = p_k \qquad \forall\, j, k \tag{8}$$

assuming stationarity [*Carle and Fogg*, 1996]. For example, hydrofacies proportions established by the vertical core data (Table 1) can be used to establish the sills for Markov chain models in nonvertical directions. In development of the transition rate matrix, row sums of unity are enforced and sills of the transition probabilities converge on the given proportions p_j for $j = 1, \cdots, N$ by maintaining

$$\sum_{k=1}^{N} r_{jk,\phi} = 0 \qquad \forall\, j \tag{9}$$

$$\sum_{j=1}^{N} p_j r_{jk,\phi} = 0 \qquad \forall\, k \tag{10}$$

[*Ross*, 1993, p. 273; *Carle and Fogg*, 1997].

4.2. Mean Lengths

Mean lengths $\bar{L}_{k,\phi}$ of a category k are readily calculated from continuous data as the total length of k in the direction ϕ divided by the total number of embedded occurrences of k along lines in the direction ϕ. Mathematically, the mean length $\bar{L}_{k,\phi}$ relates to a diagonal transition probability $t_{kk}(h_\phi)$ by

$$\frac{\partial t_{kk}(0)}{\partial h_\phi} = -\frac{1}{\bar{L}_{k,\phi}} \tag{11}$$

[*Carle and Fogg*, 1996]. Therefore the mean length will be indicated on the autotransition probability plot by the intersection of the tangent at the origin with the ordinate axis, as shown by the long-dashed lines in Figure 3. Application of (4) to (11) shows that a diagonal transition rate $r_{kk,\phi}$ directly relates to mean length by

$$r_{kk,\phi} = -(1/\bar{L}_{k,\phi}) \tag{12}$$

Estimates of mean length can be incorporated directly into (3) to establish the diagonal transition rates of a Markov chain model. Therefore knowledge of proportions and mean lengths of facies can be used to create geologically tenable models of t_{jj} in directions for which data are sparse. The length distributions generated by the Markov chain model will tend toward geometric [*Krumbein and Dacey*, 1969].

4.3. Juxtapositional Tendencies

Juxtapositional tendencies (e.g., the tendency for facies to occur adjacent to other facies) are evident in the off-diagonal transition probability plots by comparing the measured transition rates $r_{jk,\phi}$ to a theoretical transition rate $\hat{r}_{jk,\phi}$, which exhibits statistically independent juxtapositional tendencies [*Carle*, 1997b]. A resulting maximum disorder Markov chain model $\hat{t}_{jk,\phi}(\mathbf{h}_z)$ is indicated on Figure 3 by the short-dashed lines. Facies that tend to lie adjacent to each other moving from k to j in the upward direction z show measured transition probabilities greater than $\hat{t}_{jk,z}$; conversely, those that tend not

to lie adjacent to each other show measured transition probabilities less than $\hat{t}_{jk,z}$.

These juxtapositional tendencies are also reflected in the rate matrix of the Markov chain model and can be viewed relative to the mean lengths and off-diagonal independent juxtapositional tendencies as follows

$$\mathbf{R}_z = \begin{array}{c} \\ \text{gr} \\ \text{s} \\ \text{ms} \\ \text{m} \end{array} \begin{array}{c} \begin{array}{cccc} \text{gr} & \text{s} & \text{ms} & \text{m} \end{array} \\ \begin{bmatrix} -\dfrac{1}{\bar{L} = 2.00} & 5.01\hat{r} & 0.02\hat{r} & 0.03\hat{r} \\ 1.53\hat{r} & -\dfrac{1}{\bar{L} = 3.26} & 1.48\hat{r} & 0.16\hat{r} \\ 0.49\hat{r} & 0.46\hat{r} & -\dfrac{1}{\bar{L} = 1.44} & 1.39\hat{r} \\ 1.48\hat{r} & 1.43\hat{r} & 0.80\hat{r} & -\dfrac{1}{\bar{L} = 2.21} \end{bmatrix} \end{array} \tag{13}$$

The fining upward tendency, typical of fluvial deposits, is apparent from the transition rate of $5.01\hat{r}$ for gravel (gr) to sand (s) and the transition rate of $0.02\hat{r}$ and $0.03\hat{r}$ for gravel upward to muddy sand and mud, respectively, indicating that gravel was observed to transition upward primarily to sand and rarely to muddy sand or mud in the cores. The transition rate of $1.48\hat{r}$ for sand up to muddy sand (ms) and the transition rate of $0.16\hat{r}$ for the transition from sand up to mud (f) shows additional evidence of this fining upward tendency, where sand tends to transition upward to muddy sand more often than to mud.

The off-diagonal transition rates can also be interpreted in the embedded Markov chain framework, in which the transition probability from one embedded (discrete) occurrence of a facies to another is analyzed. For example, an embedded transition probability for the vertical direction would be defined as

$$\pi_{jk,z} = \Pr\{k \text{ occurs above } j|j\} \tag{14}$$

where k and j denote embedded occurrences. Most Markov analyses of geologic successions have been conducted in the embedded framework [e.g., *Doveton*, 1971; *Miall*, 1973; *Ethier*, 1975]. The off-diagonal transition rates of a spatial Markov chain can be related to the embedded transition probabilities by

$$r_{jk,\phi} = \frac{\pi_{jk,\phi}}{\bar{L}_{j,\phi}} \qquad \forall\, j \neq k \tag{15}$$

[*Carle*, 1997b]. As such, the vertical transition rate matrix could be viewed in terms of an embedded transition probability matrix as

$$\Pi_{jk,z} = \begin{array}{c} \\ \text{gr} \\ \text{s} \\ \text{ms} \\ \text{m} \end{array} \begin{array}{c} \begin{array}{cccc} \text{gr} & \text{s} & \text{ms} & \text{m} \end{array} \\ \begin{bmatrix} & 0.98 & 0.01 & 0.01 \\ 0.06 & & 0.88 & 0.06 \\ 0.03 & 0.17 & & 0.80 \\ 0.07 & 0.39 & 0.54 & \end{bmatrix} \end{array} \tag{16}$$

by applying (15) and (12) for the assumed mean lengths. Since embedded transition probabilities represent transitions between discrete occurrences of facies, the diagonal terms of $\Pi_{jk,z}$ are considered unobservable and thus left blank. Again, the fining upward tendencies in these fluvial deposits are shown by the high probability of transitioning upward from gravel to sand (0.98) rather than from gravel to muddy sand or mud (0.01 for each) and for sand up to muddy sand (0.88) rather than from muddy sand up to mud (0.06).

4.4. Markov Chain Model Development

In the vertical direction, abundant data enabled development of the model by fit to measured transition probability values; however, a Markov chain may also be readily developed from semiquantitative information on volumetric facies proportions, mean facies lengths, and estimates of juxtapositional tendencies. Application of (9) and (10) eliminates the need to specify row and column entries for one of the categories in the rate matrix. This category is referred to as the "background" category. Conceptually, the background category may be viewed as the category that "fills in the space" not occupied by other categories (e.g., fine-grained floodplain sediments). This, together with a symmetry assumption, can reduce the number of entries needed for model development to $(N^2 - N)/2$. For example, in a four-category system, only six entries in $\mathbf{R}_\phi$ may need to be established rather than 16.

Importantly, a Markov chain model produced as described above honors basic probability laws. In contrast, previous indicator coregionalization models that neglect cross correlations or rely only on empirical curve fitting can lead to significant "order relation violations" (i.e., cumulative probability distribution functions that are not monotonically increasing or are outside the interval [0, 1]) [*Journel and Posa*, 1990] and problems maintaining consistency with prescribed proportions when applied in (co)kriging or simulation [e.g., *Goovaerts*, 1996].

5. Lateral Model Development: Soil Map Analysis

The soil survey, when mappable units are characterized as previously described (Figure 2), provides the basis for development of models of subsurface lateral spatial variability. However, during this model development, key differences between the surface and subsurface facies distributions must be considered. First, gravel exists in the subsurface but is not seen on the soil map over most of the alluvial fan since gravel exists below the sand facies as channel lag deposits. Therefore parameters related to gravel distribution must be estimated from geologic inference based on distributions of the other facies.

Second, the subsurface facies proportions differ from the surface facies proportions because of varying preservation potential of the different facies. Preservation potential refers to the probability that a deposit remains intact during subsequent erosion and burial. In the case of the Kings River alluvial fan, channel migration across the fan removed fine-grained bar top and floodplain sediments and replaced them with coarse-grained channel deposits. This resulted in higher sand proportions and lower mud proportions in the subsurface than those measured on the soil survey. Therefore volumetric proportions from the USGS core data were used in lateral model development. Climatic change, causing source area changes, could be interpreted as a cause for this change in proportions; however, sedimentologic and geomorphic evidence suggests that both the surface and subsurface sediments were deposited on the alluvial fan during past glacial episodes [*Huntington*, 1980; *Lettis*, 1988].

Finally, measurements from the soil survey used in the analysis were made only in younger portions of the fan where eolian reworking and pedogenic alteration of facies were minimal. By focusing transition probability measurements on areas that were deposited within a relatively limited time span (e.g., during the most recent glacial cycle), incorrect cross correlations over major unconformity boundaries were avoided. Additionally, by limiting measurements where effects of subsequent sediment modification are minimal, the soil survey measurements most closely reflect the lateral facies distribution from fan deposition.

Models of lateral facies distributions developed in other studies have been derived by Walther's law concepts [e.g., *Carle and Fogg*, 1997; *Carle et al*., 1998] or through covariance measurements made between widely spaced wells. However, the soil survey provides a strong advantage over either of these approaches because the lateral facies distributions observed on the soil survey reflect expected subsurface distributions more directly. Direct application of Walther's law may be problematic in a fluvial setting, where vertical distributions may not adequately reflect lateral relationships because of erosion and truncation of facies higher in a sequence. When using well data, the spacing between wells is often greater than the correlation range; therefore measured data tend to be scattered, and the model fit is prone to error. The soil survey provides a clearer image of lateral facies distributions prior to burial and therefore a reasonable "training image" of lateral variability in the subsurface.

6. Lateral Direction Models and Parameter Estimation

In the interpreted soil survey (Figure 2), facies appear to be symmetrically distributed (e.g., one facies does not appear to be preferentially distributed on one side or the other of a different facies); therefore an assumption of facies symmetry in lateral directions is reasonable. Given this assumption, use of mud as the background category, and application of (9) and (10), only six parameters are required to develop the Markov chain model in each lateral direction (depositional dip and strike): mean lengths for gravel, sand, and muddy sand and juxtapositional tendency parameters for gravel → sand, gravel → muddy sand, and sand → muddy sand. Of these six parameters, mean lengths for sand and muddy sand and the transition rates for sand → muddy sand were derived directly from measurements of the soil survey data. The remaining three parameters were estimated from geologic inference based on the observed soil survey and subsurface facies distributions. Volumetric proportions used to set the sills of the transition rate matrices were taken from core measurements. The sections 6.1–6.3 describe how these parameters were determined.

6.1. Mean Lengths

Mean lengths for the sand and muddy sand were measured directly from the soil survey. The trend of channel axes tends to be variable, but, generally, axes radiate outward from an apex. Consequently, mean lengths were measured manually along multiple transects made parallel to the apparent channel trends for the depositional dip direction and perpendicular to channel axes for the depositional strike direction. Measurements from 340 transects on the soil map show that sand facies lengths, measured along straight lines, are approximately 1500 m and 625 m for depositional dip and strike, respectively, and muddy sand lengths are approximately 800 m and 400 m, for depositional dip and strike, respectively. Experience has shown that these lengths produce channels in the conditional simulations which appear as connected as those seen in the soil survey map.

Since gravel occurs below the sand as lag deposits and is not observed on the soil survey map, the mean length values for gravel cannot be interpreted directly from the soil survey. However, because gravel is found primarily within the sand facies, the mean length of gravel must be less than that of sand. Channel lag gravels also tend to be oriented in a similar manner to that of the channel trend, as indicated by the sand facies. These observations are supported by facies models developed for fluvial settings [*Miall*, 1992, 1996]. Therefore a reasonable estimate of gravel length would be less than sand lengths, with anisotropy similar to the sand facies. Gravel mean lengths of 650 m and 200 m were chosen for depositional dip and strike, respectively, in the Markov chain model since these lengths represent the maximum gravel lengths along the principle directions that produced a reasonable Markov chain model (e.g., positive transition probabilities and appropriate juxtapositional tendency values for the background category discussed in section 6.2).

6.2. Juxtapositional Tendency Parameters

In order to determine the transition rates for sand → muddy sand, transition probability measurements from a 30.5 m grid over an 18 km^2 area of the fan were made directly from the soil survey map along depositional dip and strike. The 18 km^2 area was chosen because depositional strike and dip trends were consistent throughout the area, soils within the area represent deposits of a single glacial period, and minimal eolian modification is present. A Markov chain model fit to these measurements provided embedded transition probability values for the sand → muddy sand transition ranging from 0.31 to 0.48. The higher value of 0.48 was used because this resulted in embedded transition probability values for the sand → mud and muddy sand → mud transitions that reasonably matched those measured in the soil survey. Modeled probability values for transitions to mud were lower than those measured on the soil survey because less mud is preserved in the subsurface.

Because the gravel facies was not present on the soil map, the related transition rates were developed by geologic inference. Gravel occurs in strong association with the sand facies, as shown by its position in the core and through its interpretation as a channel lag deposit. Therefore high probability of occurrence should be reflected in the embedded transition probability for the gravel → sand transition. Likewise, facies models indicate that lag gravel only occurs adjacent to muddy sand and mud on the channel margins at locations where the channel eroded into these fine-grained facies. Therefore the embedded transition probabilities for gravel → muddy sand and gravel → mud should be relatively low. Thus embedded transition probability values of 0.70 and 0.15 were chosen for the gravel → sand and gravel → muddy sand transitions, respectively (making the embedded transition probability for gravel → mud also equal to 0.15). Though these specific values for the gravel transitions contain some uncertainty, they produce a reasonable model that is consistent with fluvial facies models [e.g., *Miall*, 1992, 1996] where sand and gravel facies are strongly associated and gravel transitions laterally to the finer-grained facies only in relatively rare instances.

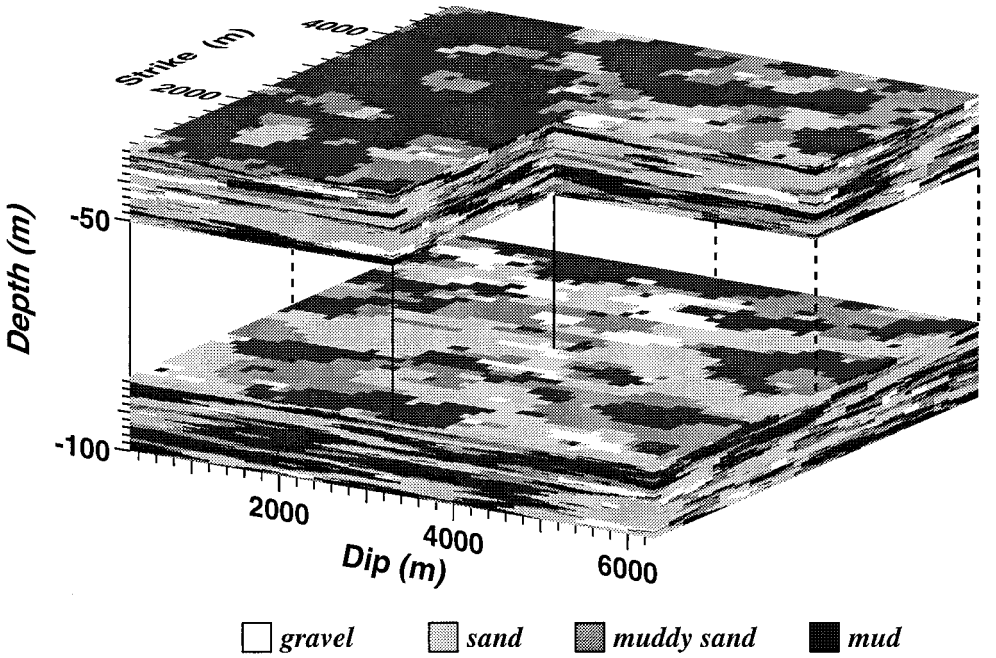

Figure 4. A geostatistical realization of a portion of the Kings River alluvial fan produced by conditional sequential indicator simulation and simulated quenching based on the three-dimensional Markov chain model.

6.3. Final Lateral Models

The Markov chain models developed for lateral variability in the Kings River alluvial fan deposits based on these six parameters in terms of embedded transition probabilities are

$$\Pi_{jk,\mathrm{DIP}} = \begin{array}{c} \\ \mathrm{gr} \\ \mathrm{s} \\ \mathrm{ms} \\ \mathrm{m} \end{array} \begin{array}{c} \begin{array}{cccc} \mathrm{gr} & \mathrm{s} & \mathrm{ms} & \mathrm{m} \end{array} \\ \begin{bmatrix} \bar{L} = 650 & 0.70 & 0.15 & b \\ s & \bar{L} = 1500 & 0.48 & b \\ s & s & \bar{L} = 800 & b \\ b & b & b & b \end{bmatrix} \end{array} \tag{17}$$

$$\Pi_{jk,\mathrm{STRIKE}} = \begin{array}{c} \\ \mathrm{gr} \\ \mathrm{s} \\ \mathrm{ms} \\ \mathrm{m} \end{array} \begin{array}{c} \begin{array}{cccc} \mathrm{gr} & \mathrm{s} & \mathrm{ms} & \mathrm{m} \end{array} \\ \begin{bmatrix} \bar{L} = 200 & 0.70 & 0.15 & b \\ s & \bar{L} = 625 & 0.48 & b \\ s & s & \bar{L} = 400 & b \\ b & b & b & b \end{bmatrix} \end{array} \tag{18}$$

where b indicates background category entry and s indicates an entry symmetrical to the opposite entry (e.g., gravel → sand is symmetrical to sand → gravel, etc.). Symmetrical entries were calculated through application of

$$r_{jk,\phi} = (p_k/p_j) r_{kj,\phi} \tag{19}$$

and background category entries were determined through application of (9) and (10).

7. Three-Dimensional Modeling and Simulation

A complete three-dimensional Markov chain model is developed by ellipsoidal interpolation of the models for the three principal directions: strike, dip, and vertical [*Carle and Fogg*, 1997]. This three-dimensional Markov chain model is then used in sequential indicator simulation (SIS) followed by simulated quenching or "zero temperature" annealing [*Carle*, 1996, 1997a] to generate a geostatistical realization of subsurface facies distribution in the northern portion of the Kings River alluvial fan (Figure 4). This realization was conditioned on core, well log, and C horizon texture data. Importantly, the soil survey provided directional information used to align the principal model directions along depositional strike and dip during simulation; thus the realization shown in Figure 4 has facies oriented along directions consistent with the local geology.

The conditional SIS algorithm is identical to the algorithm described by *Deutsch and Journel* [1992], except that kriging based on indicator covariances is replaced with cokriging based on transition probabilities. SIS alone does not adequately preserve the cross correlations contained in the coregionalization model, but it does provide an excellent starting point for the simulated quenching step. The simulated quenching produces realizations that honor the coregionalization model without adding much computational burden [*Carle*, 1997a].

A close inspection of the realization from a portion of the Kings River alluvial fan (Figure 4) reveals that observed geologic tendencies, including fining upward tendencies and elongate channels, are evident in the realization.

8. Closing Remarks

Typical hydrogeologic data sets consisting of widely spaced boreholes usually provide only sketchy information on the lateral distribution of hydrofacies. However, soil surveys may provide, in effect, an outcrop map indicative of the lateral heterogeneity patterns in alluvial aquifer systems. Channel orientations and geometries, as well as channel, levee, and floodplain juxtapositional tendencies are recorded by the soil survey. Through collective analysis of surface and subsurface data and knowledge of the geologic processes, a representative subsurface coregionalization model was constructed using the transition probability geostatistical method. Models developed

for use in the geostatistical simulation contain plausible geometric factors consistent with all the data and geologic concepts. Without the soil mapping, one would have only a vague notion of the lateral heterogeneity present in the subsurface for model development.

In the example application to the Kings River alluvial fan, transition probability measurements from the soil survey could not be blindly related to parameters used to develop a three-dimensional subsurface Markov chain model. Adjustments for subsurface preservation of facies must be incorporated into the models. Additionally, lengths and juxtapositional tendencies related to the gravel facies could not be directly estimated from the soil survey, leaving some level of uncertainty. However, geometries and associations of the gravel facies to other facies, as indicated by published facies models [e.g., *Miall*, 1992, 1996] along with channel geometries estimated from the soil survey provide a reasonable estimate of these parameters. Minor variation of gravel lengths or juxtaposition parameters have little effect on the overall simulated structure. Additionally, these uncertainties can help provide focus for additional data collection efforts.

Soil survey data may provide additional utility beyond geostatistical model development. Information about facies distributions and geometry from the soil survey may also help direct data collection by giving indications of ideal locations for future well drilling or geophysical survey sites. Additionally, the soil surveys can provide a qualitative check for other geometrical or process-imitating model results.

The high quality of the soil survey for eastern Fresno County [*Huntington*, 1971] helped ensure successful application of these data to the geostatistical analysis. Increased application of soil maps in hydrogeologic characterizations, as well as increased efforts to map C horizon textures overlying alluvial aquifers, is clearly warranted. The potential for hydrogeologic application well below the root zone provides compelling motivation for focusing greater resources and effort on soil mapping, with particular attention paid to parent material lithology as reflected by the C horizon.

Through use of a transition probability/Markov approach [*Carle*, 1996, 1997b; *Carle and Fogg*, 1996, 1997; *Carle et al.*, 1998] the geological features observed in the soil survey and well data are preserved in the geostatistical realizations of the aquifer. In particular, geologically plausible juxtapositional relationships, such as fining upward tendencies, are readily modeled using either raw data or semiquantitative information. The resulting realizations provide much improved, geologically tenable models of subsurface hydraulic heterogeneity for use in groundwater flow and contaminant transport modeling.

Notation

$\mathbf{h}$	separation lag vector.
k, j	categories or facies.
K	hydraulic conductivity.
$\bar{L}$	mean category (facies) length.
N	number of categories.
p	category (facies) proportions.
r	transition rate values.
$\mathbf{R}$	transition rate matrix.
t	transition probability.
$\mathbf{T}$	transition probability matrix.
$\pi_{jk,\phi}$	embedded transition probability.

Acknowledgments. This material is based upon work supported by the Cooperative State Research Service, U.S. Department of Agriculture, under Agreement 93-38420-8792, Occidental Chemical Company, the Geological Society of America (research grant 5736-95), Lawrence Livermore National Laboratory, N.I.E.H.S. Superfund grant ES-04699, U.S. Environmental Protection Agency grant R819658, Center for Ecological Health Research at University of California at Davis, and the U.S. Army Waterways Experiment Station. This work would not have been possible without the data and insights provided by K. R. Burow and the U.S. Geological Survey. We also benefited greatly from discussions with Gordon Huntington, Thomas Harter, Eric LaBolle, David VanBrocklin, Jeffrey Mount, Michael Singer, and Randy Southard.

References

Agterberg, F. P., *Geomathematics*, 596 pp., Elsevier Sci., New York, 1974.

Bashore, W. M., U. G. Araktingi, M. Levy, and W. J. Schweller, Importance of a geological framework and seismic data integration for reservoir modeling and subsequent fluid-flow predictions, in *Stochastic Modeling and Geostatistics: Principles, Methods, and Case Studies*, *AAPG Comput. Appl. Geol.*, vol. 3, edited by J. M. Yarus and R. L. Chambers, pp. 159–175, Am. Assoc. of Pet. Geol., Tulsa, Okla., 1994.

Burow, K. R., G. S. Weissmann, R. D. Miller, and G. Placzek, Hydrogeologic facies characterization of an alluvial fan near Fresno, California, using geophysical techniques, *U.S. Geol. Surv. Open File Rep.*, *97-46*, 15 pp., 1997.

Carle, S. F., A transition probability-based approach to geostatistical characterization of hydrostratigraphic architecture, Ph.D. dissertation, 182 pp., Univ. of Calif., Davis, 1996.

Carle, S. F., Implementation schemes for avoiding artifact discontinuities in simulated annealing, *Math. Geol.*, *29*(2), 231–244, 1997a.

Carle, S. F., Integration of geologic interpretation into geostatistical simulation, in *IAMG '97*, *Proceedings of the Third Annual Conference of the International Association for Mathematical Geology*, edited by V. Pawlowsky Glahn, pp. 711–716, Int. Assoc. for Math. Geol., Barcelona, Spain, 1997b.

Carle, S. F., and G. E. Fogg, Transition probability-based indicator geostatistics, *Math. Geol.*, *28*(4), 453–476, 1996.

Carle, S. F., and G. E. Fogg, Modeling spatial variability with one- and multi-dimensional continuous Markov chains, *Math. Geol.*, *29*(7), 891–918, 1997.

Carle, S. F., E. M. LaBolle, G. S. Weissmann, D. VanBrocklin, and G. E. Fogg, Conditional simulation of hydrofacies architecture: A transition probability/Markov approach, in *Hydrogeologic Models of Sedimentary Aquifers*, *SEPM Concepts in Hydrogeol. Environ. Geol.*, vol. 1, edited by G. S. Fraser and J. M. Davis, pp. 147–170, Soc. for Sediment. Geol., Tulsa, Okla., 1998.

Dagan, G., *Flow and Transport in Porous Formations*, 465 pp., Springer-Verlag, New York, 1989.

Desbarats, A. J., Geostatistical analysis of interwell transmissivity in heterogeneous aquifers, *Water Resour. Res.*, *29*, 1239–1246, 1993.

Deutsch, C. V., and A. G. Journel, *GSLIB*, *Geostatistical Software Library and User's Guide*, 340 pp., Oxford Univ. Press, New York, 1992.

Doveton, J. H., An application of Markov chain analysis to the Ayrshire Coal measures succession, *Scott. J. Geol.*, *7*(1), 11–27, 1971.

Ethier, V. G., Application of Markov analysis to the Banff Formation (Mississippian), Alberta, *Math. Geol.*, *7*(1), 47–61, 1975.

Fogg, G. E., C. D. Noyes, and S. F. Carle, Geologically-based model of heterogeneous hydraulic conductivity in an alluvial setting, *Hydrogeol. J.*, *6*, 131–143, 1998.

Gelhar, L. W., and C. L. Axness, Three-dimensional stochastic analysis of macrodispersion in aquifers, *Water Resour. Res.*, *19*, 161–180, 1983.

Goovaerts, P., Stochastic simulation of categorical variables using a classification algorithm and simulated annealing, *Math. Geol.*, *28*(7), 909–921, 1996.

Huntington, G. L., *Soil Survey, Eastern Fresno Area, California*, U.S. Dep. of Agric., U.S. Gov. Print. Off., 323 pp., Washington, D. C., 1971.

Huntington, G. L., Soil-land form relationships of portions of the San Joaquin River and Kings River alluvial depositional systems in the Great Valley of California, Ph.D. dissertation, 147 pp., Univ. of Calif., Davis, 1980.

Hyndman, D. W., and S. M. Gorelick, Estimating lithologic and transport properties in three dimensions using seismic and tracer data, the Kesterson aquifer, *Water Resour. Res.*, *32*, 2659–2670, 1996.

Johnson, N. M., and S. J. Dreiss, Hydrostratigraphic interpretation using indicator geostatistics, *Water Resour. Res.*, *25*, 2501–2510, 1989.

Journel, A. G., and D. Posa, Characteristic behavior and order relations for indicator variograms, *Math. Geol.*, *22*(8), 1011–1025, 1990.

Koltermann, C. E., and S. M. Gorelick, Heterogeneity in sedimentary deposits: A review of structure-imitating, process-imitating, and descriptive approaches, *Water Resour. Res.*, *32*, 2617–2658, 1996.

Krumbein, W. C., and M. F. Dacey, Markov chains and embedded Markov chains in geology, *Math. Geol.*, *1*(1), 79–96, 1969.

Lettis, W. R., Quaternary geology of the northern San Joaquin Valley, in *Studies of the Geology of the San Joaquin Basin*, edited by S. A. Graham, *SEPM Publ.*, *60*, pp. 333–351, Pac. Sect., Soc. for Sediment. Geol., Santa Barbara, Calif., 1988.

McKenna, S. A., and E. P. Poeter, Simulating geological uncertainty with imprecise data for groundwater flow and advective transport modeling, *in* Yarus, Y. M., and R. L. Chambers (Eds.), *Stochastic Modeling and Geostatistics: Principles, Methods, and Case Studies*, *AAPG Comput. Appl. Geol.*, vol. 3, edited by J. M. Yarus and R. L. Chambers, pp. 241–248, Am. Assoc. of Pet. Geol., Tulsa, Okla., 1994.

McKenna, S. A., and E. P. Poeter, Field example of data fusion in site characterization, *Water Resour. Res.*, *31*, 3229–3240, 1995.

Miall, A. D., Markov chain analysis applied to an ancient alluvial plain succession, *Sedimentology*, *20*(3), 347–364, 1973.

Miall, A. D., Fluvial facies models, in *Facies Models: Response to Sea Level Change*, 2nd ed., edited by R. G. Walker and N. P. James, pp. 119–142, Geol. Assoc. of Can., St. John's, Newfoundland, Can., 1992.

Miall, A. D., *The Geology of Fluvial Deposits*, 582 pp., Springer-Verlag, New York, 1996.

Neuman, S. P., and D. Zhang, Considerations of scale and information content in subsurface flow and transport modeling, in *Joint U.S. Geological Survey*, *U.S. Nuclear Regulatory Commission Workshop on Research Related to Low-Level Radioactive Waste Disposal*, *Water Resour. Invest.*, edited by P. R. Stevens and T. J. Nicholson, *U.S. Geol. Surv. Water Resour. Invest. Rep.*, *WRI 95-4015*, 136–149, 1996.

North, C. P., The prediction and modelling of subsurface fluvial stratigraphy, in *Advances in Fluvial Dynamics and Stratigraphy*, edited by P. A. Carling and M. R. Dawson, pp. 395–508, John Wiley, New York, 1996.

Ritzi, R. W., Jr., D. F. Dominic, N. R. Brown, K. W. Kausch, P. J. McAlenney, and M. J. Basial, Hydrofacies distribution and correlation in the Miami Valley aquifer system, *Water Resour. Res.*, *31*, 3271–3281, 1995.

Ross, S., *Introduction to Probability Models*, 5th ed., 556 pp., Academic, San Diego, Calif., 1993.

S. F. Carle, Lawrence Livermore National Laboratory, Livermore, CA.

G. E. Fogg and G. S. Weissmann, Hydrologic Sciences, University of California, Davis, One Shields Avenue, Davis, CA 95616-8628. (gweissmann@ucdavis.edu)

(Received June 29, 1998; revised December 17, 1998; accepted February 12, 1999.)